Resveratrol ameliorates high-fat diet-induced insulin resistance via the DDIT4/mTOR pathway in skeletal muscle

XINYAN PAN[1,2], GANGQIANG XUE[3], MING ZHAO[4], ZIPING XIANG[2,5], DIAN LIU[5], ZESEN DUAN[5] and CHAO WANG[2]

[1]Department of Endocrinology, Hebei General Hospital, Shijiazhuang, Hebei 050051, P.R. China; [2]Key Laboratory of Metabolic Diseases, Hebei General Hospital, Shijiazhuang, Hebei 050051, P.R. China; [3]Department of Pharmaceutic Preparation, The Fourth Hospital of Shijiazhuang City, Shijiazhuang, Hebei 050011, P.R. China; [4]Clinical Laboratory, Hebei General Hospital, Shijiazhuang, Hebei 050051, P.R. China; [5]Graduate School, North China University of Science and Technology, Tangshan, Hebei 063210, P.R. China

Received August 9, 2024; Accepted March 24, 2025

DOI: 10.3892/br.2025.1977

Abstract. Resveratrol (RSV) is a natural ingredient used in the treatment of diabetes mellitus. However, the antidiabetic mechanism of RSV is not clear. In the present study the antidiabetic mechanism of RSV was investigated using mice with high-fat diet (HFD)-induced insulin resistance (IR). C57BL/6J mice were divided into the following three groups: Control (CON), HFD, and HFD + RSV (RSV, 100 mg/kg body weight/day). Mice were administered RSV for 6 weeks; then biochemical and histological parameters, as well as gene and protein expression were detected. Compared with the CON group, the circulating levels of blood glucose, insulin, triglycerides, total cholesterol and high-density lipoprotein cholesterol, and area under the glucose curve were increased ($P<0.05$), the quantitative insulin sensitivity check index was decreased ($P<0.05$), and lipid accumulation in skeletal muscle was increased in the HFD group. RSV treatment was able to reverse this process and promote the IRS-1/PI3K/AKT/GLUT4 signaling pathway. Moreover, DNA damage-inducible transcript 4 (DDIT4) expression was upregulated, while the expression levels of mammalian target of rapamycin (mTOR) and p70 ribosomal protein S6 kinase were downregulated in the HFD + RSV group compared with the HFD group ($P<0.05$). Cell experiments inhibiting DDIT4 or activating mTOR also confirmed the role of these pathways. In summary, RSV ameliorated IR and glucose as well as lipid metabolism, and promoted the IRS-1/PI3K/AKT/GLUT4 signaling pathway through the DDIT4/mTOR signaling pathway in mice with HFD-induced IR.

Correspondence to: Dr Chao Wang, Key Laboratory of Metabolic Diseases, Hebei General Hospital, 348 Heping West Road, Shijiazhuang, Hebei 050051, P.R. China
E-mail: cwyx163@163.com

Abbreviations: RSV, resveratrol; IR, insulin resistance; DDIT4, DNA-damage-inducible transcript 4; mTOR, mammalian target of rapamycin; p70S6K, p70 ribosomal protein S6 kinase; IRS-1, insulin receptor substrate-1; AKT, protein kinase B; PI3K, phosphatidylinositol 3-kinase; GLUT4, glucose transporter type 4; TG, triglyceride

Key words: insulin resistance, resveratrol, PI3K, AKT, GLUT4, DDIT4, mTOR

Introduction

In recent years, the use of Traditional Chinese medicine to improve metabolic diseases has gradually become a research focus. Among numerous natural hypoglycemic active ingredients, investigators have paid increasing attention to resveratrol (RSV), which is a polyphenolic plant antitoxin belonging to the stilbene family, widely found in grapes and other plants, and has hypoglycemic activity (1). The mechanism of RSV in reducing insulin resistance (IR) involves the regulation of multiple signal transduction pathways, such as silent mating type information regulation 2 homolog-1/peroxisome proliferator-activated receptor γ coactivator-1α, inhibitor of κB kinase/nuclear factor κB inhibitor/nuclear factor κB, adenosine phosphate kinase (AMPK) and phosphatidylinositol 3-kinase (PI3K)/protein kinase B (AKT)/endothelial nitric oxide synthase pathways (2). The in-depth study of these signaling pathways has clarified some molecular mechanisms of the effects of RSV (2). In insulin target tissues, skeletal muscle accounts for 70-80% of the total glucose intake stimulated by insulin, thus playing a crucial role in regulating systemic glucose homeostasis (3).

The mammalian target of rapamycin (mTOR) is a serine/threonine protein kinase with highly conserved structure and function belonging to the PI3K family. mTOR-mediated signaling pathways play crucial roles in metabolism, immunity, growth, development, aging as well as other physiological processes (4). Research has shown that mTOR signaling is also involved in the occurrence and development of numerous metabolic diseases, such as diabetes, hyperlipidemia and osteoporosis (4). A previous study found that mTOR functions as a nutrient receptor, and that the mTOR signal was activated in various tissues of a high-fat diet (HFD) or obese rodents (5), and was closely related to the occurrence and development of IR (6,7). Skeletal muscle anabolism is

driven by numerous stimuli such as growth factors, nutrients (including amino acids and glucose), and mechanical stress. These stimuli are integrated by the mechanistic target of mTOR signal transduction cascade (8).

The DNA-damage-inducible transcript factor 4 (DDIT4) plays a role in insulin signal transduction, DNA damage repair, nutritional deprivation, oxidative metabolism, endoplasmic reticulum stress and the hypoxia response (9-14). Some studies have found that DDIT4 is involved in nutritional metabolism, and is crucial to insulin-mediated activation of AKT and mTOR (15-17). However, at present, there are few reports regarding the actions of DDIT4 involving the mTOR pathway during IR. Notably, changes in DDIT4 mRNA and protein have been observed in skeletal muscle under various physiological conditions (such as nutrient consumption and resistance exercise) and pathological conditions (including sepsis, alcoholism, diabetes and obesity) suggesting a role for DDIT4 in regulating mTOR-dependent skeletal muscle protein metabolism (18).

In the present study, RSV was administered to C57BL/6J mice with IR induced by an HFD to observe the effect of RSV on insulin and mTOR signaling pathways as well as DDIT4, and to explore the mechanism of the RSV-mediated reduction of IR, to further understand the specific functions of RSV in glucose and lipid metabolism.

Materials and methods

Animal experiments. A total of 33 healthy 6-week-old male C57BL/6J mice weighing ~22 g were purchased from the Hebei Invivo Biotechnology Co., Ltd. (license no. SCXK 2023-002) and raised in the barrier system of the animal room at the Clinical Research Center of Hebei General Hospital (Shijiazhuang, China). The humidity was controlled at 40-60% with a room temperature at 20-25˚C with a standard 12-h light-dark cycle. A week after adaptive feeding, mice were randomly divided into the following two groups: Control group (CON, n=11) and HFD group (n=22). The CON group was given an ordinary diet (D12450J: 70% carbohydrate, 20% protein, 10% fat, 3.85 kcal/g), and the HFD group was given an HFD (D12492J: 20% carbohydrate, 20% protein, 60% fat, 5.24 kcal/g) (19). All feeds were purchased from Beijing Huafukang Biotechnology Co., Ltd. After 8 weeks of an HFD, mice were fasted overnight (12 h) and then underwent an intraperitoneal glucose tolerance test (IPGTT) (19). The tail tip blood glucose was measured at point 0 using Roche rapid glucose meter test strips, followed by intraperitoneal injection of 50% glucose injection at 2 g/kg (20-22). Then, the tail tip blood glucose values were measured at 15, 30, 60 and 120 min using Roche rapid glucose meter test strips after glucose treatment. The amount of blood used for measuring blood glucose with a blood glucose meter was approximately 20 μl per mouse at each time point (20-22). The area under the glucose curve (AUC) was calculated (23); IPGTT-AUC=0.125 x BG0 + 0.25 x BG15 + 0.375 x BG30 + 0.75 x BG60 + 0.5 x BG120 (BGx=blood glucose values at different time points) (23). Eleven mice were randomly selected from the HFD group to form the high-fat feeding with RSV intervention group (HFD + RSV group), and were administered 100 mg/kg body weight RSV by gavage for 6 weeks (24), while other mice in the HFD group and the CON group were admnistered 0.9% sodium chloride solution containing 0.1% DMSO by gavage.

After 6 weeks of treatment, IPGTT was performed again to detect the blood glucose value of each mouse at each time point, and then the calculated AUC was used to evaluate the degree of IR. All three groups of mice were intraperitoneally injected with 1.5 units of insulin (Merck KGaA)/40 g body weight, and then anesthetized by intraperitoneal injection of 2% pentobarbital sodium at a dose of 40 mg/kg. After 20 min, blood samples collected by cardiac puncture were centrifuged at 1,500 x g for 10 min at 4˚C. The serum was collected and stored at -80˚C for the subsequent determination of serological indicators. Cervical dislocation caused rapid unconsciousness and death with minimal distress to the mice, and was a humane way to euthanize the mice. Then, skeletal muscle samples were quickly removed and stored in liquid nitrogen for subsequent research. The present study was approved (approval no. 2023-LW-055) by the Ethics Committee of Hebei General Hospital (Shijiazhuang, China).

Serological indicators. Detection kits for total cholesterol (TC; cat. no. A111-1-1), triglyceride (TG; cat. no. A110-1-1), low-density lipoprotein-cholesterol (LDL-C; cat. no. A113-1-1) and high-density lipoprotein-cholesterol (HDL-C; cat. no. A112-1-1) were acquired from the Nanjing Jiancheng Bioengineering Institute in accordance with the manufacturer's instructions. Insulin concentrations were obtained using an ELISA kit from ALPCO (cat. no. 80-INSMSU-E01) in accordance with the manufacturer's instructions. The Qualitative Insulin Sensitivity Check Index (QUICKI) was determined according to the equation: QUICKI=1/[log(I0) + log(G0)] (25), with I0=fasting insulin and G0=fasting glucose.

Histological assessment of skeletal muscle tissue. The skeletal muscle tissues of mice were fixed in 4% paraformaldehyde at 4˚C for 6 h. Then, the samples were dehydrated using a conventional alcohol gradient, clarified using xylene, embedded in paraffin and cut into 5-μm slices. The sections were then stained with an H&E Stain Kit (cat. no. G1005; Wuhan Servicebio Technology Co., Ltd.) using hematoxylin and eosin solutions for 5 min staining each at room temperature. A Modified Oil Red O Stain Kit (cat. no. G1261; Beijing Solarbio Science & Technology Co. Ltd.) was used to detect lipid droplets in skeletal muscle sections, which were stained with Modified Oil Red O Stain Solution (included in the aforementioned kit) for 10 min at 25˚C, and then stained with Mayer's Hematoxylin Solution (included in the aforementioned kit) for 1 min at 25˚C. The staining of sections was completed according to the manufacturer's protocol, and stained sections were examined under a light microscope (magnification, x400).

C2C12 cell culture. The C2C12 mouse myoblast cell line (cat. no. CL-0044; Procell Life Science & Technology Co., Ltd.) was cultured in culture medium (cat. no. CM-0044 Procell Life Science & Technology Co., Ltd.) until the cells reached 70-80% confluence. The differentiation medium (cat. no. PM150210A; Procell Life Science & Technology Co., Ltd.) and 2% horse serum (cat. no. 164215; Procell Life Science & Technology Co., Ltd.) were used to induce differentiation of C2C12 cells. Mycoplasma contamination was not detected in

the cells. Differentiated C2C12 cells were then incubated with 0.5 mM palmitic acid (PA; cat. no. 800508; Merck KGaA) for 24 h, designated the PA group. RSV (cat. no. R817263-5g; Shanghai Macklin Biochemical Technology Co. Ltd.) was added to the medium at concentrations of 30 μM at room temperature to form the PA + RSV group. Some of the PA + RSV group cells were again divided into two groups: The PA + RSV + MHY1485 group C2C12 cells were treated with 10 μM MHY1485 (cat. no. HY-B0795; MedChemExpress) to activate mTOR, and the PA + RSV + DDIT4-siRNA group C2C12 cells were transfected with a small interfering (si)RNA against DDIT4 (DDIT4-siRNA; Shanghai Genechem Co. Ltd.), all incubated at 37˚C for 24 h. The cells were collected for western blotting and cellular TG content determination.

Transfection with siRNAs. Shanghai Genechem Co., Ltd. provided three DDIT4-siRNAs (DDIT4-siRNA-1: Sense strand, 5'-GGGAAGGAAGUGUUCUCCAGGAAGU-3' and antisense strand, 5'-ACUUCCUGGAGAACACUUCCUUCC C-3'; DDIT4-siRNA-2: Sense strand, 5'-GCAGCUGCUCAU UGAAGAGUGUUGA-3' and antisense strand, 5'-UCAACA CUCUUCAAUGAGCAGCUGC-3'; DDIT4-siRNA-3: Sense strand, 5'-GGUGCCCAUGUACUGGAGGAUUCAA-3' and antisense strand, 5'-UUGAAUCCUCCAGUACAUGGGCAC C-3'), along with a negative control siRNA (sense strand, 5'-GGUCUUACGUCAGUCACAAUAUCUG-3' and antisense strand, 5'-CAGAUAUUGUGACUGACGUAAGACC-3'). To prepare the RNA oligonucleotide stock solution, 20 pmol of siRNA was mixed with 50 μl of Opti-MEM I reduced serum medium (cat. no. 31985-062; Thermo Fisher Scientific, Inc.) and stored at -20˚C. Additionally, 1 μl of Lipofectamine® 2000 (cat. no. 11668019; Invitrogen; Thermo Fisher Scientific, Inc.) was diluted in 50 μl of Opti-MEM I medium. For experiments, the RNA oligonucleotide stock solution and the diluted Lipofectamine 2000 solution were mixed to prepare transfection complexes at room temperature. Cells were seeded into 24-well plates once they reached ~40% confluence at 37˚C. Transfection was performed when the cells reached ~60% confluence, with 100 μl siRNA transfection complexes at a concentration of 50 nM added to each well and incubated at 37˚C for 24 h. Western blotting was performed 24 h after transfection to assess the efficiency of the different siRNAs and determine the most effective one for future experiments. The optimal siRNA was determined to be DDIT4-siRNA-1.

TG assay. Cellular TG content was measured using a TG detection kit (cat. no. ab65336; Abcam Plc) according to the manufacturer's instructions.

Glucose content in culture medium. The glucose oxidase assay kit (cat. no. E1010-500; Beijing Applygen Gene Technology Co., Ltd.) was used to measure the remaining glucose content in culture medium as per the manufacturer's instructions.

Reverse transcription-quantitative polymerase chain reaction (RT-qPCR). Total RNA from mouse skeletal muscle tissues was extracted using Trizol reagent [ref. no. DP424; Tiangen Biotech (Beijing) Co. Ltd.] and was reverse-transcribed into cDNA using a Fastking RT Kit [ref. no. KR116; Tiangen Biotech (Beijing) Co. Ltd.] for qPCR. RNA was tested for purity and concentration using NanoDrop® 2000 (Thermo Fisher Scientific, Inc.). Amplification was performed using the SuperReal PreMix Plus (SYBR Green) [ref. no. GFP205; Tiangen Biotech (Beijing) Co. Ltd.] in an Applied Biosystems 7500 Real-Time PCR System (Thermo Fisher Scientific, Inc.). The cycling conditions were as follows: 3 min of pre-denaturation at 95˚C, then 5 sec at 95˚C, and 32 sec at 60˚C, with 41 cycles in total. The melting point curve was established at 60-95˚C. The expression levels of PI3K, insulin receptor substrate (IRS)-1, AKT, glucose transporter type 4 (GLUT4), mTOR, p70 ribosomal protein S6 kinase (p70S6K/S6K1) and DDIT4 mRNA in skeletal muscle tissue were evaluated. β-actin was used as the internal reference control for genes. Relative gene expression levels were quantified by the $2^{-\Delta\Delta Cq}$ method (26). The specific primers involved in the study are listed in Table I.

Western blotting. Skeletal muscle samples were added to 0.5 ml of pre-cooled lysate at 4˚C, and then homogenized and stored at 4˚C overnight. Subsequently, the tissue homogenate was centrifuged at 16,200 x g at 4˚C for 15 min and the supernatants were collected. C2C12 cells were lysed in RIPA lysis buffer (cat. no. C1053-100; Applygen Technologies, Inc.) to extract total cellular proteins. The same amounts of protein (~50 μg/lane) for different group samples were separated by sodium dodecyl sulfate-polyacrylamide gel electrophoresis (5% resolving gel, 10% stacking gel), and then transferred to polyvinylidene fluoride membranes, which were blocked in 5% skimmed milk at room temperature for 2 h. The membranes were then incubated with the primary antibodies at 4˚C overnight at the following concentrations: Phosphorylated (p)-IRS-1 (rabbit antibody; 1:1,000; cat. no. ab5599; Abcam Ltd.), total (t)-IRS-1 (rabbit antibody; 1:1,000; cat. no. ab52167; Abcam Ltd.), p-AKT (rabbit antibody; 1:1,000; cat. no. AA329; Beyotime Institute of Biotechnology), t-AKT (rabbit antibody; 1:1,000; cat. no. AA326; Beyotime Institute of Biotechnology), p-PI3K (rabbit antibody; 1:1,000; cat. no. AF5905; Beyotime Institute of Biotechnology), t-PI3K (rabbit antibody; 1:1,000; cat. no. 20583-1-AP; Proteintech Group, Inc.), GLUT4 (rabbit antibody; 1:3,000; cat. no. ab65267; Abcam Ltd.), DDIT4 (rabbit antibody; 1:2,000; cat. no. AF5147; Beyotime Institute of Biotechnology), p-mTOR (rabbit antibody; 1:4,000; cat. no. ab109268; Abcam Ltd.), t-mTOR (rabbit antibody; 1:4,000; cat. no. ab32028; Abcam Ltd.), p-p70S6K (rabbit antibody; 1:1,000; cat. no. ab59208; Abcam Ltd.), t-p70S6K (rabbit antibody; 1:2,000; cat. no. ab32529; Abcam Ltd.), and β-actin (rabbit antibody; 1:5,000; cat. no. 20536-1-AP; Proteintech Group Inc.). After three washes with Tris-buffered saline, the membranes were incubated with horseradish peroxidase-conjugated secondary antibodies (anti-rabbit; 1:5,000; cat. no. S0001; Affinity Biosciences) for 2 h at room temperature. Finally, the washed membranes were immersed in chemiluminescence solution (cat. no. 34580; Thermo Fisher Scientific, Inc.) for 2 min, and images were acquired using a Gel Imager System (GDS8000; UVP, Inc.). The Alpha software processing system (AlphaEaseFC 4.0; ProteinSimple) was used to measure the optical densities of the target bands.

Statistical analyses. The SPSS v22.0 (IBM, Inc.) was used for data analysis. The results are presented as the mean ± standard deviation (SD). Independent sample t-test was used

Table I. Primers used for real-time quantitative polymerase chain reaction.

Gene	Primer	Sequence (5'-3')
PI3K	Forward	5'-CCCATGGGACAACATTCCAA-3'
	Reverse	5'-CATGGCGACAAGCTCGGTA-3'
AKT	Forward	5'-TCAGGATGTGGATCAGCGAGA-3'
	Reverse	5'-CTGCAGGCAGCGGATGATAA-3'
IRS-1	Forward	5'-GCACCTGGTGGCTCTCTACAC-3'
	Reverse	5'-TCGCTATCCGCGGCAAT-3'
GLUT4	Forward	5'-GTGACTGGAACACTGGTCCTA-3'
	Reverse	5'-CCAGCCACGTTGCATTGTAG-3'
DDIT4	Forward	5'-TACTGCCCACCTTTCAGTTG-3'
	Reverse	5'-GTCAGGGACTGGCTGTAACC-3'
mTOR	Forward	5'-GCGGCCTGGAAATGCGGAAGTGG-3'
	Reverse	5'-AAAGCCCCAAGGAGCCCCAACA-3'
p70S6K	Forward	5'-CACTCAGGCCCCCCTACACT-3'
	Reverse	5'-GCCGTCACTGAAAACCAAGTTC-3'
β-actin	Forward	5'-GGTGGGAATGGGTCAGAAGG-3'
	Reverse	5'-AGGTCTCAAACATGATCTGGGT-3'

PI3K, phosphatidylinositol 3-kinase; AKT, protein kinase B; IRS-1, insulin receptor substrate-1; GLUT4, glucose transporter 4; DDIT4, DNA damage-inducible transcript 4; mTOR, mammalian target of rapamycin; p70S6K, p70 ribosomal protein S6 kinase.

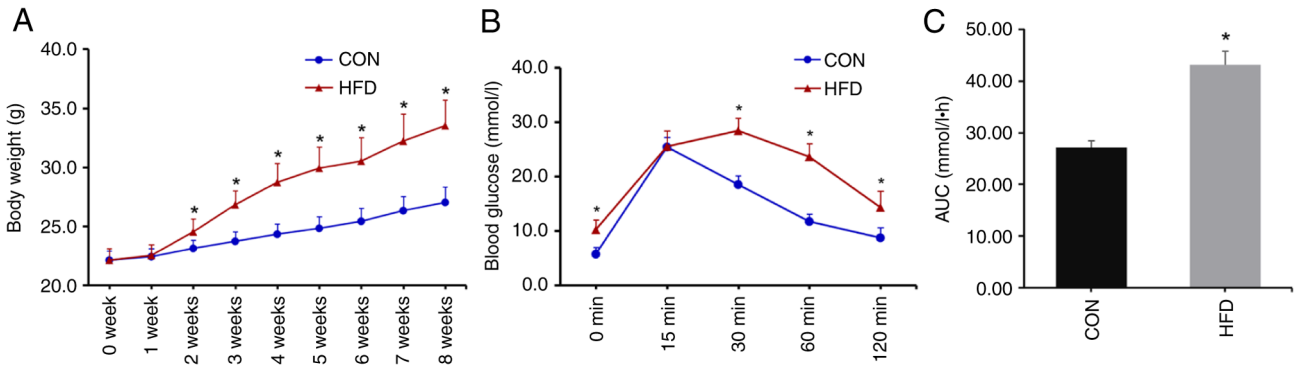

Figure 1. Body weight and intraperitoneal glucose tolerance testing data after diet consumption for 8 weeks. (A) Body weight of the CON and HFD groups. (B) Blood glucose concentrations at different time points of the intraperitoneal glucose tolerance test. (C) AUC for glucose. Data are presented as the mean ± SD (n=11, CON group; n=22, HFD group). Student's t-test was used for statistical analysis. *P<0.05 vs. the CON group. CON, control; HFD, high-fat diet; AUC, area under the curve.

to analyze two normally distributed sample comparisons. One-way ANOVA was used for statistical analysis followed by the Bonferroni's multiple comparison test or Tamhane's multiple comparison test. P<0.05 was considered to indicate a statistically significant difference. Each experiment was performed in triplicate to ensure reliability and reproducibility of the results.

Results

Establishment of the C57BL/6J mouse model with HFD-induced IR. There were no differences in initial body weights between the CON and HFD groups. From the second week of high-fat feeding, the body weights of mice in the HFD group were significantly higher than in the CON group (Fig. 1A). The IPGTT was performed after 8 weeks of diet consumption. After fasting for 12 h, there was no difference in weight loss between the two groups (Table II). Blood glucose levels in the HFD group were significantly higher at 0, 30, 60 and 120 min than corresponding levels in the CON group (Fig. 1B). Compared with the CON group, the AUC was significantly increased in the HFD group (Fig. 1C), indicating that the IR model was successfully established.

Effects of RSV administration on body weight and blood glucose, insulin, as well as lipid levels in mice with IR. Following high-fat feeding, the body weight of the HFD group was significantly higher than that in the CON group. After RSV administration for 4 weeks, the body weight of the HFD + RSV group was lower than that in the HFD group (Fig. 2A).

Table II. Weight loss in mice after 12 h of fasting.

Groups	First fasting for 12 h		Second fasting for 12 h		
	CON group (n=11)	HFD group (n=22)	CON group (n=11)	HFD group (n=11)	HFD + RSV group (n=11)
Weight loss (g)	2.6±0.2	2.7±0.2	3.4±0.2	3.7±0.3	3.6±0.4
t/F	1.353			2.655	
P-value	0.186			0.087	

CON, control; HFD, high-fat diet.

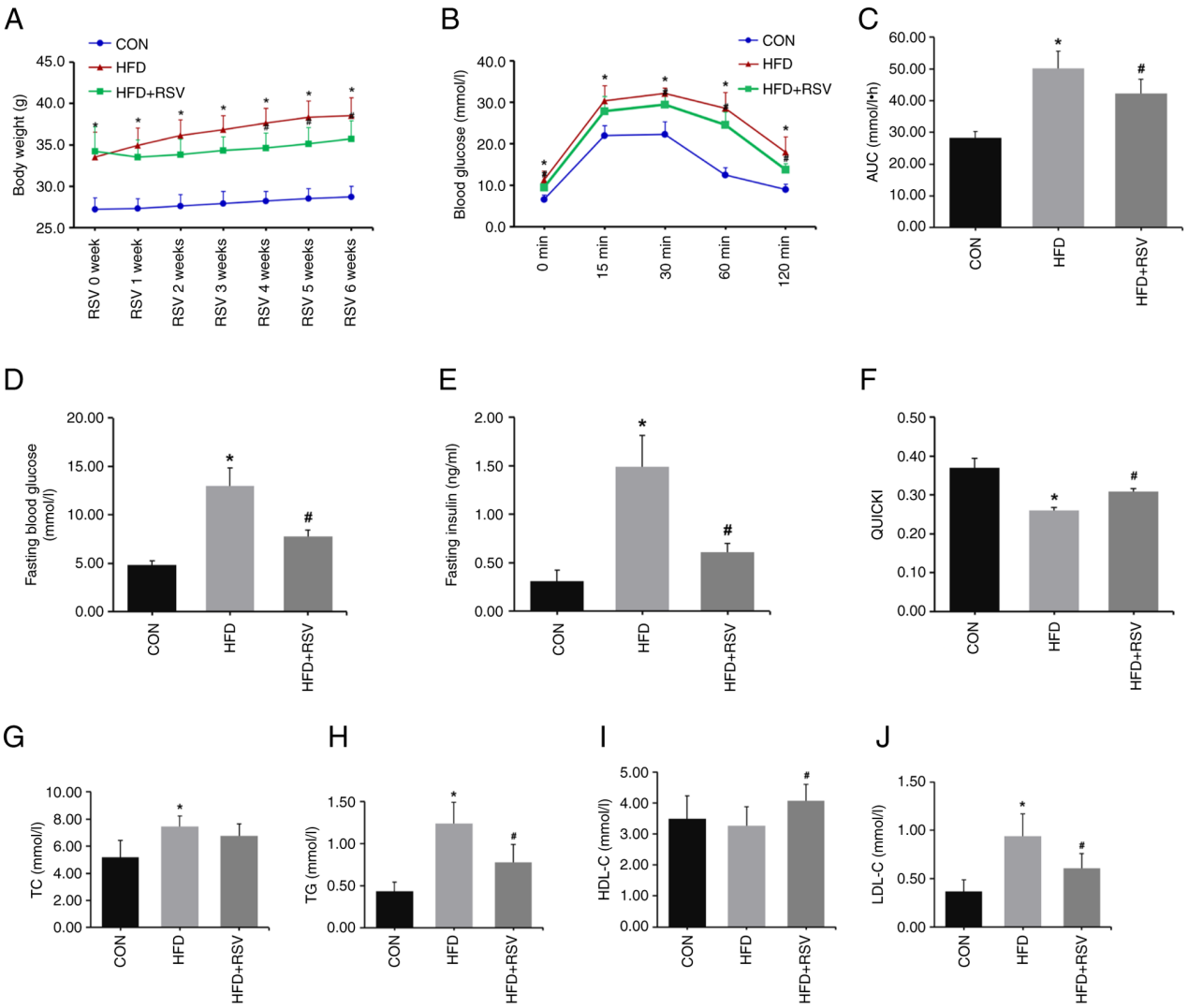

Figure 2. Effects of RSV on body weight, and blood glucose, as well as insulin and lipid levels in mice with insulin resistance. (A) Body weight of mice with RSV treatment for 6 weeks. (B) The levels of blood glucose at 0, 15, 30, 60 and 120 min of the intraperitoneal glucose tolerance test after RSV administration for 6 weeks. (C) AUC of glucose. (D) Fasting blood glucose. (E) Fasting insulin. (F) QUICKI value. (G) TC level. (H) TG level. (I) HDL-C level. (J) LDL-C level. Data are presented as the mean ± SD (n=11). One-way ANOVA, followed by Bonferroni's or Tamhane's multiple comparison post hoc tests, were used for statistical analysis. *P<0.05 vs. the CON group; #P<0.05 vs. the HFD group. RSV, resveratrol; AUC, area under the curve; QUICKI, Qualitative Insulin Sensitivity Check Index; TC, total cholesterol; TG, triglyceride; HDL-C, high-density lipoprotein-cholesterol; LDL-C, low-density lipoprotein-cholesterol; CON, control; HFD, high-fat diet.

The IPGTT test was performed on three groups of mice after 6 weeks of treatment with RSV. After fasting for 12 h, there was no difference in weight loss among the three groups (Table II). The experiment determined that the maximum percentage of body weight loss that was observed in the study was 10.6% after fasting for 12 h. Compared with the CON

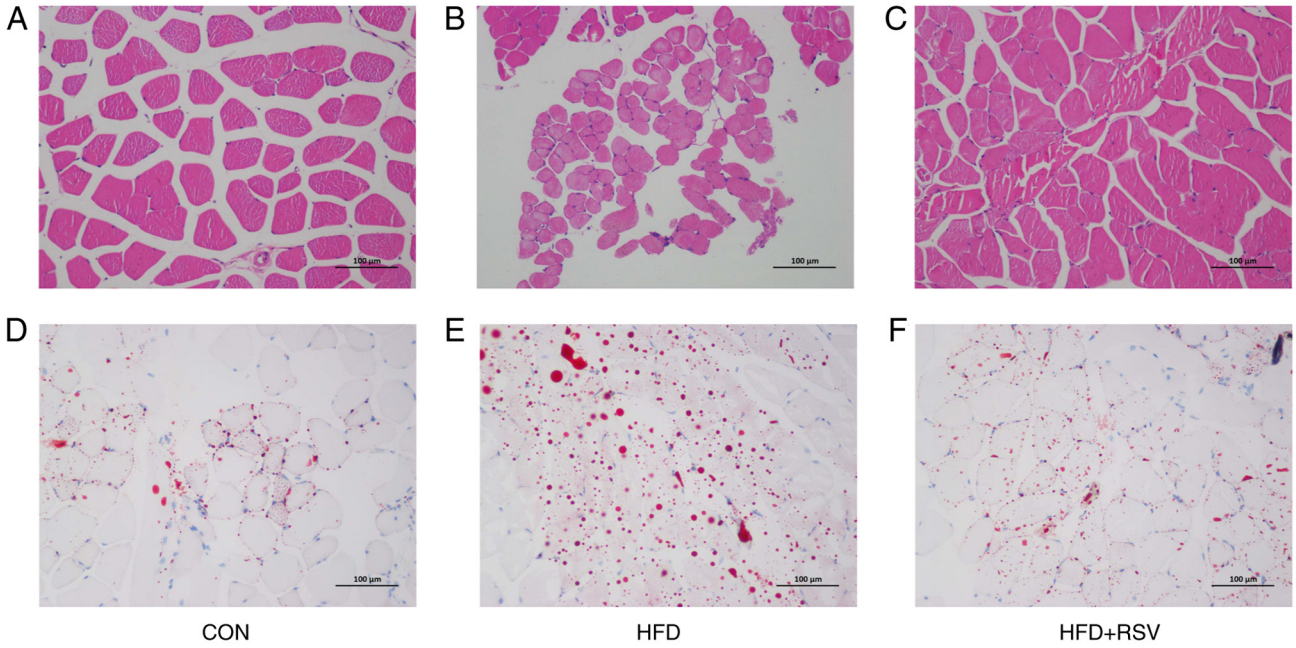

Figure 3. Effects of RSV on skeletal muscle histopathology of mice on an HFD. (A-C) Hematoxylin and eosin staining and (D-F) Oil red O staining. (A-F) Magnification, x400; scale bar, 100 μm. HFD, high fat diet; CON, control; RSV, resveratrol.

group, blood glucose levels were higher at 0, 15, 30, 60 and 120 min (Fig. 2B), and the AUC was increased in the HFD group (Fig. 2C). Compared with the HFD group, blood glucose levels were lower at 0, 30, 60 and 120 min, with no difference at 15 min (Fig. 2B), and the AUC was significantly decreased in the HFD + RSV group (Fig. 2C).

Compared with the CON group, the fasting blood glucose and insulin levels were significantly higher (Fig. 2D and E), and the QUICKI value was lower in the HFD group (Fig. 2F). Compared with the HFD group, fasting blood glucose and insulin levels were significantly lower (Fig. 2D and E), and the QUICKI value was higher in the HFD + RSV group (Fig. 2F). These data indicated that RSV may significantly ameliorate the IR of HFD-fed mice.

In addition, serum concentrations of TG, TC and LDL-C were significantly increased in the HFD group compared with the CON group (Fig. 2G, H and J). Compared with the HFD group, TG and LDL-C were significantly decreased, and HDL-C was significantly higher in the HFD + RSV group, with no statistical difference in TC levels between the two groups (Fig. 2G-J).

Effects of RSV on histology and lipid accumulation in skeletal muscle of mice with IR. The H&E staining revealed normal histology of skeletal muscle cells in the CON group (Fig. 3A). However, in the HDF group, the cellular structure of skeletal muscle cells was fuzzy and disordered, with fat drop vacuoles of different sizes in the cytoplasm, constricting the nuclei, which were closer to the outer cell membrane (Fig. 3B). In the HFD + RSV group, the morphology of skeletal muscle cells resembled morphological features between those of the CON and HFD groups, with lipid droplet vacuoles significantly reduced compared with those in the HFD group (Fig. 3C). Oil Red O staining showed larger numbers of red fat droplets in skeletal muscle cells of the HFD group compared with the CON group (Fig. 3D and E). The number of red fat droplets in skeletal muscle cells of the HFD + RSV group was decreased compared with the HFD group, and was between the numbers found in the CON and HFD groups (Fig. 3D-F).

Effects of RSV on mRNA and protein expression levels of insulin signaling pathway factors in skeletal muscle tissue of mice with IR. There were no differences in the mRNA expression levels of IRS-1, PI3K and AKT in skeletal muscle from the three groups of mice (Fig. 4A-C). In the HFD group, the expression level of GLUT4 mRNA was significantly decreased compared with the CON group (Fig. 4D). Compared with the HFD group, the expression level of GLUT4 mRNA was upregulated in the HFD + RSV group (Fig. 4D).

Western blotting showed that there were no differences in the total protein expression levels of IRS-1, PI3K and AKT in skeletal muscle from the three groups (Fig. 5A). Compared with the CON group, the expression levels of p-PI3K, p-AKT and GLUT4 were decreased, while the expression of p-IRS-1 was increased in the HFD group (Fig. 5A and E). Moreover, the phosphorylated protein-to-total protein ratios for PI3K and AKT were downregulated, while that for IRS-1 was upregulated, in the HFD vs. the CON groups (Fig. 5B-D). Compared with the HFD group, the protein expression levels of p-PI3K, p-AKT and GLUT4 were increased, while the expression of p-IRS-1 was decreased in the HFD + RSV group (Fig. 5A and E). Furthermore, the phosphorylated protein-to-total protein ratios for PI3K and AKT were upregulated, while that for IRS-1 was downregulated, in the HFD + RSV group relative to the HFD group (Fig. 5B-D). These data suggested that administration of RSV in mice with IR could activate the IRS-1/PI3K/AKT/GLUT4 signaling pathway.

Effects of RSV on mRNA and protein expression levels of DDIT4, mTOR and p70S6K in skeletal tissue of mice with IR. Compared with CON mice, the mRNA and protein expression

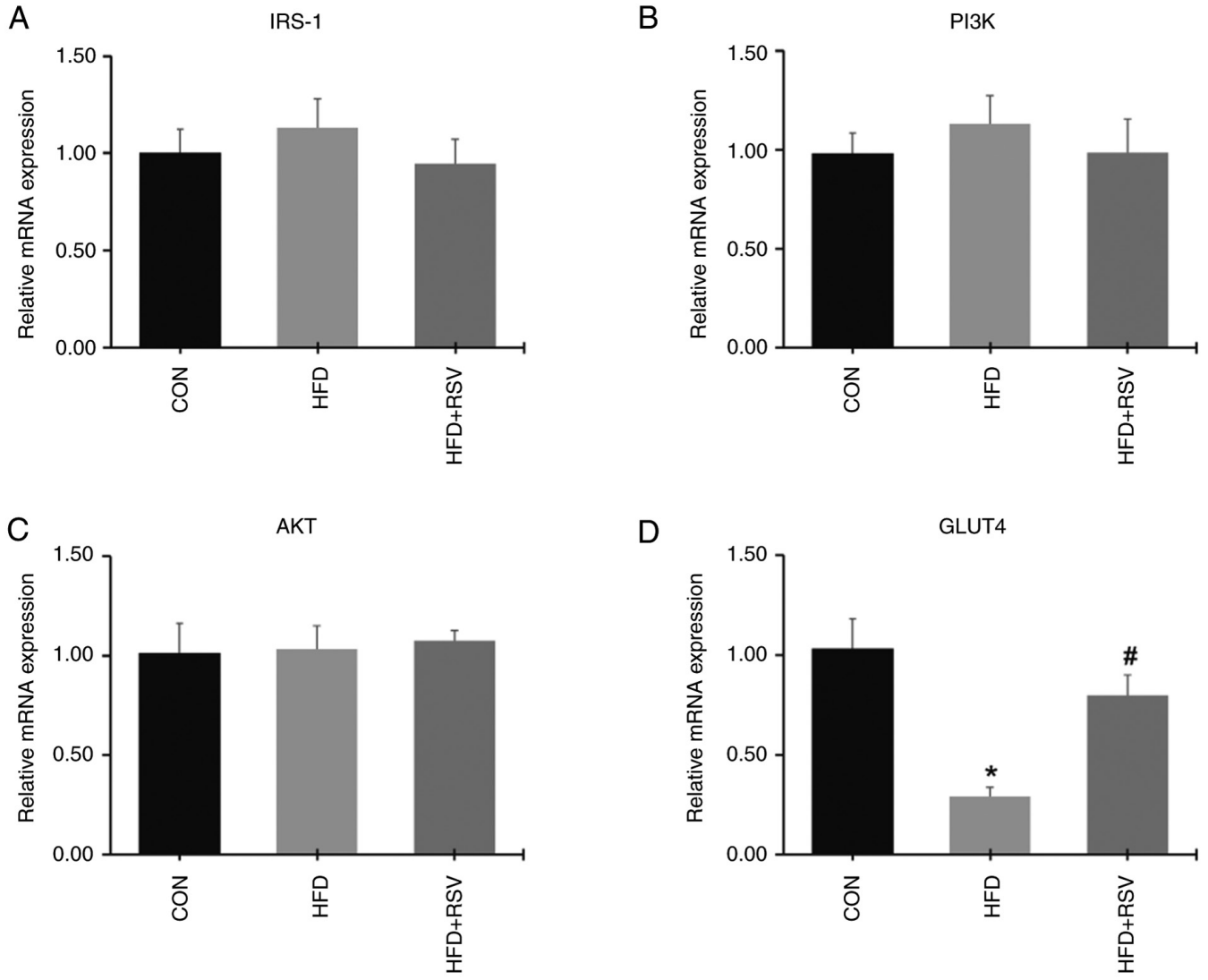

Figure 4. Effect of RSV on the expression levels of IRS-1, PI3K, AKT and GLUT4 mRNA in skeletal tissue. (A) IRS-1, (B) PI3K, (C) AKT and (D) GLUT4 mRNA levels. Data are presented as the mean ± SD (n=11). *P<0.05 vs. the CON group; #P<0.05 vs. the HFD group. RSV, resveratrol; IRS-1, insulin receptor substrate-1; PI3K, phosphatidylinositol 3-kinase; AKT, protein kinase B; GLUT4, glucose transporter 4; CON, control; HFD, high-fat diet.

levels of DDIT4 in skeletal muscle were significantly decreased in the HFD mice (Fig. 6A-C), indicating that the expression of DDIT4 was decreased under the IR conditions induced by the HFD. However, the mRNA and protein expression levels of DDIT4 in skeletal muscle were increased in the HFD + RSV group compared with the HFD group, indicating that RSV promotes the expression of DDIT4 in mice with IR.

Compared with the CON group, the mRNA expression levels of mTOR and p70S6K in skeletal muscle tissue were significantly increased in the HFD group. However, the mRNA expression levels of mTOR and p70S6K in skeletal muscle were significantly decreased in the HFD + RSV group compared with the HFD group (Fig. 7A and B).

Western blotting results showed that the expression levels of total and phosphorylated mTOR and p70S6K proteins in skeletal muscle tissue were increased in the HFD group compared with the CON group (Fig. 7C). The expression levels of total and phosphorylated mTOR and p70S6K proteins in skeletal muscle from the HFD + RSV group were significantly decreased compared with the HFD group (Fig. 7C and E). Furthermore, RSV reduced the increasing trend of the phosphorylated protein-to-total protein ratios for mTOR and p70S6K induced by the HFD (Fig. 7D and E). These findings indicated that RSV inhibited the expression levels of mTOR and p70S6K in mice with IR.

Expression of DDIT4, mTOR, PI3K, AKT, and GLUT4 in MHY1485-treated C2C12 cells. Compared with those in the PA group, the protein expression levels of DDIT4, p-PI3K/t-PI3K, p-AKT/t-AKT and GLUT4 were increased, whereas those of p-mTOR/t-mTOR were decreased in the PA + RSV group (Fig. 8A and B). There were no differences in the protein expression levels of DDIT4 between the PA + RSV group and PA + RSV + MHY1485 group (Fig. 8A and B). Compared with the PA + RSV group, the protein expression levels of p-PI3K/t-PI3K, p-AKT/t-AKT and GLUT4 were decreased, whereas those of p-mTOR/t-mTOR were increased in the PA + RSV + MHY1485 group (Fig. 8A and B). Compared with the PA group, the glucose concentration was significantly decreased in the culture medium from the PA + RSV group (Fig. 8C).

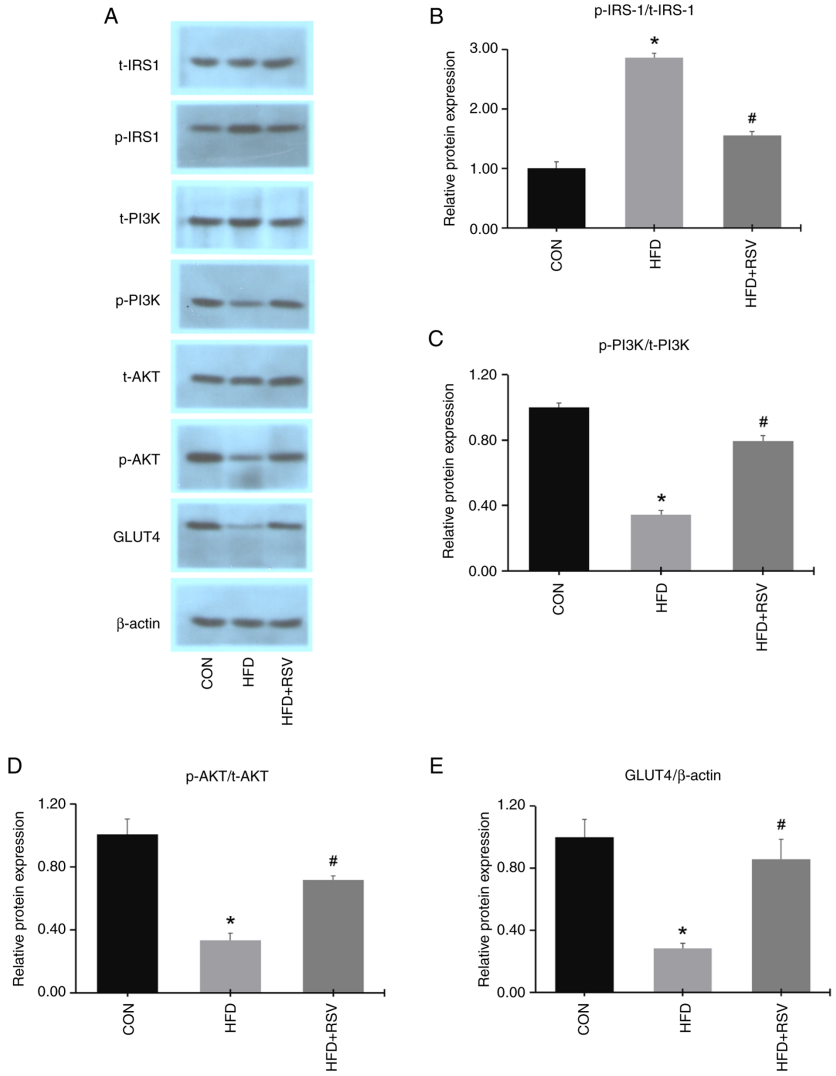

Figure 5. Effects of RSV on the protein expression levels of insulin signaling pathway factors in skeletal muscle. (A) Bands of various insulin signaling pathway proteins. (B) p-IRS-1/t-IRS-1, (C) p-PI3K/t-PI3K, (D) p-AKT/t-AKT and (E) GLUT4/β-actin protein expression levels. Data are presented as the mean ± SD (n=11). *P<0.05 vs. the CON group; #P<0.05 vs. the HFD group. RSV, resveratrol; p-, phosphorylated; t-, total; IRS-1, insulin receptor substrate-1; PI3K, phosphatidylinositol 3-kinase; AKT, protein kinase B; GLUT4, glucose transporter 4; CON, control; HFD, high-fat diet.

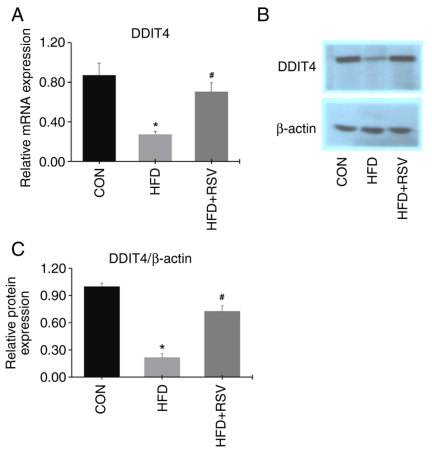

Figure 6. Effects of RSV on the mRNA and protein expression levels of DDIT4 in skeletal muscle. (A) Relative mRNA expression of DDIT4. (B) Protein bands of DDIT4. (C) DDIT4/β-actin protein expression levels. Data are presented as the mean ± SD (n=11). *P<0.05 vs. the CON group; #P<0.05 vs. the HFD group. RSV, resveratrol; DDIT4, DNA-damage-inducible transcript 4; CON, control; HFD, high-fat diet.

Compared with the PA + RSV group, the glucose concentration was significantly increased in the culture medium from the PA + RSV + MHY1485 group (Fig. 8C). The TG content was decreased in the PA + RSV group cells compared with those in the PA group (Fig. 8D). The TG content was increased in the PA + RSV + MHY1485 group cells compared with those in the PA + RSV group (Fig. 8D).

Expression of DDIT4, mTOR, PI3K, AKT, and GLUT4 in C2C12 cells with silencing of DDIT4. Plasmid validation experiments revealed that DDIT4-siRNA-1 had the most significant silencing effect (Fig. 9A). The cells were then divided into four groups: CON, PA, PA + RSV, and PA + RSV + DDIT4 siRNA groups.

Compared with the PA + RSV group, the protein expression levels of DDIT4, p-PI3K/t-PI3K, p-AKT/t-AKT and GLUT4 were decreased, whereas those of p-mTOR/t-mTOR were increased in the PA + RSV + DDIT4-siRNA group (Fig. 9B and C). Compared with the PA + RSV group, the glucose concentration in the culture medium and TG content

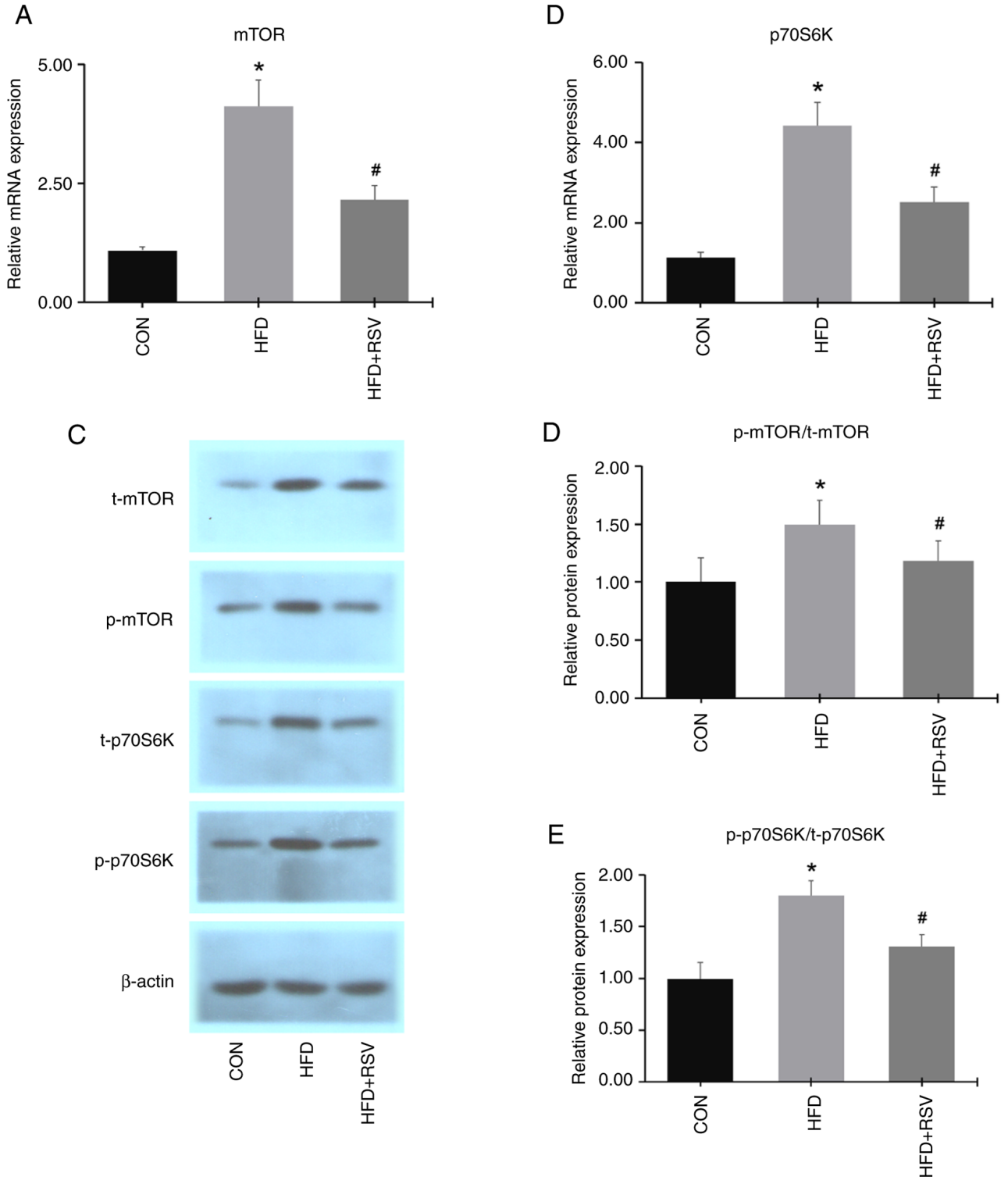

Figure 7. Effects of RSV on the mRNA and protein expression levels of mTOR and p70S6K in skeletal muscle. (A) mRNA expression of mTOR. (B) mRNA expression of p70S6K. (C) Protein bands of mTOR and p70S6K. (D) p-mTOR/t-mTOR and (E) p-p70S6K/t-p70S6K protein expression levels. Data are presented as the mean ± SD (n=11). *P<0.05 vs. the CON group; #P<0.05 vs. the HFD group. RSV, resveratrol; mTOR, mammalian target of rapamycin; p70S6K, p70 ribosomal protein S6 kinase; p-, phosphorylated; t-, total; CON, control; HFD, high-fat diet.

of the cells were increased in the PA + RSV + DDIT4-siRNA group (Fig. 9D and E).

The results showed that RSV could activate DDIT4 expression, thereby inhibiting the mTOR pathway and then reducing IR and lipid deposition in high-fat induced C2C12 cells (Fig. 10).

Discussion

In the present study, a mouse model with IR was established by an HFD. This model closely simulated manifestations of IR, including weight gain, hyperglycemia, hyperlipidemia, impaired glucose tolerance and a low QUICKI index. In the

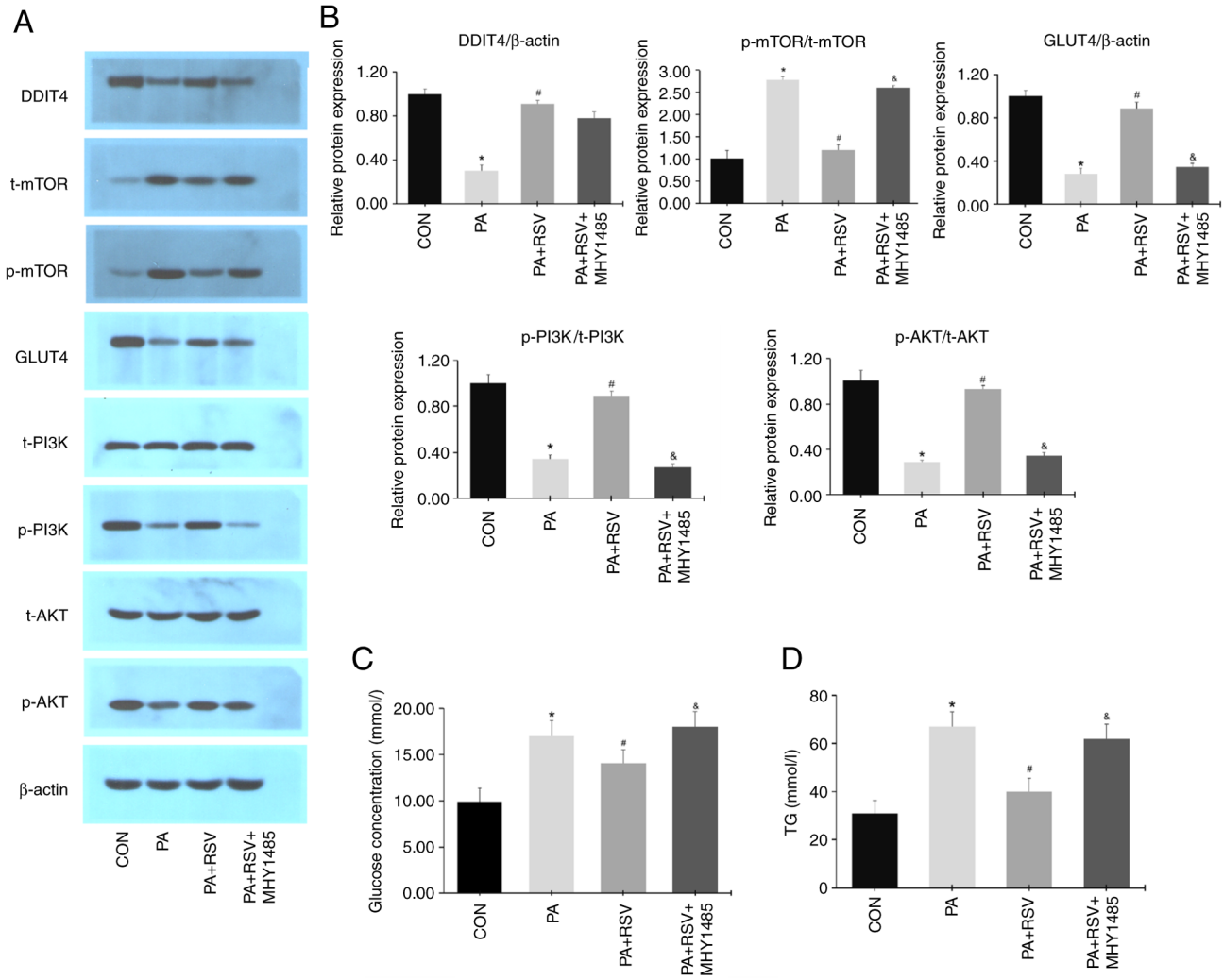

Figure 8. Expression of DDIT4, mTOR, GLUT4, PI3K, and AKT in MHY1485-treated IR C2C12 cells. (A) Protein expression levels of DDIT4, mTOR, GLUT4, PI3K, AKT after the activation of mTOR. (B) Semi-quantification of p-protein/t-protein ratios for mTOR, PI3K, AKT and protein expression levels of DDIT4, GLUT4 after MHY1485 treatment. (C) Glucose levels in culture medium after MHY1485 treatment. (D) Cell TG levels after MHY1485 treatment. Data are presented as the mean ± SD (n=3). *P<0.05 vs. the CON group; $^{\#}$P<0.05 vs. the PA group; $^{\&}$P<0.05 vs. the PA + RSV group. DDIT4, DNA-damage-inducible transcript 4; mTOR, mammalian target of rapamycin; GLUT4, glucose transporter 4; PI3K, phosphatidylinositol 3-kinase; AKT, protein kinase B; IR, insulin resistance; p-, phosphorylated; t-, total; TG, triglyceride; CON, control; PA, palmitic acid; RSV, resveratrol.

present study, treatment with RSV markedly reduced the concentration of blood lipid and glucose, and decreased the AUC of IPGTT and body weight of mice with HFD-induced IR. RSV also increased the QUICKI index, improved the morphology and structure of skeletal muscle tissue, and significantly reduced lipid droplet vacuoles in skeletal muscle cells. It was determined that there was no difference in weight loss among the groups after fasting for 12 h with a maximum weight loss of 10.6%, which was similar to the results found in another study (27). These results showed that RSV reduced IR and lipid deposition in the skeletal muscle of mice fed an HFD. Cell experiments also confirmed that PA intervention could reduce glucose uptake and increase lipid levels in C2C12 cells. RSV could reverse this condition, while the mTOR agonist MHY1485 or siRNA against DDIT4 intervention further confirmed that RSV inhibited mTOR by activating DDIT4, thereby affecting the activation of the insulin pathway. Previous research also revealed that RSV plays a beneficial role in glucose and lipid metabolism in animal models and individuals with obesity and type 2 diabetes mellitus (28-30), and reduced IR in various models (30,32).

To determine the molecular mechanism of the effects of RSV, the present study examined gene and protein expression levels of PI3K, AKT and GLUT4 in murine skeletal muscle and C2C12 cells. Biologically, insulin can combine with the insulin receptor of peripheral target organs, such as skeletal muscle, and then interact with IRS to activate the PI3K/AKT signaling pathway, resulting in the downstream translocation of GLUT4 to the cell membrane, thereby increasing glucose uptake and metabolism in peripheral target organs (33). RSV can increase the expression of GLUT4 in peripheral tissues by activating the PI3K/AKT signaling pathway, thereby increasing tissue uptake of glucose and lowering blood glucose levels (34,35). Similarly, the present study found that an HFD inhibited the IRS-1/PI3K/AKT/GLUT4 insulin signaling pathway. However, RSV partially corrected the aberrant protein levels of PI3K, AKT and GLUT4 in mice with IR, suggesting that RSV exerts a regulatory effect by

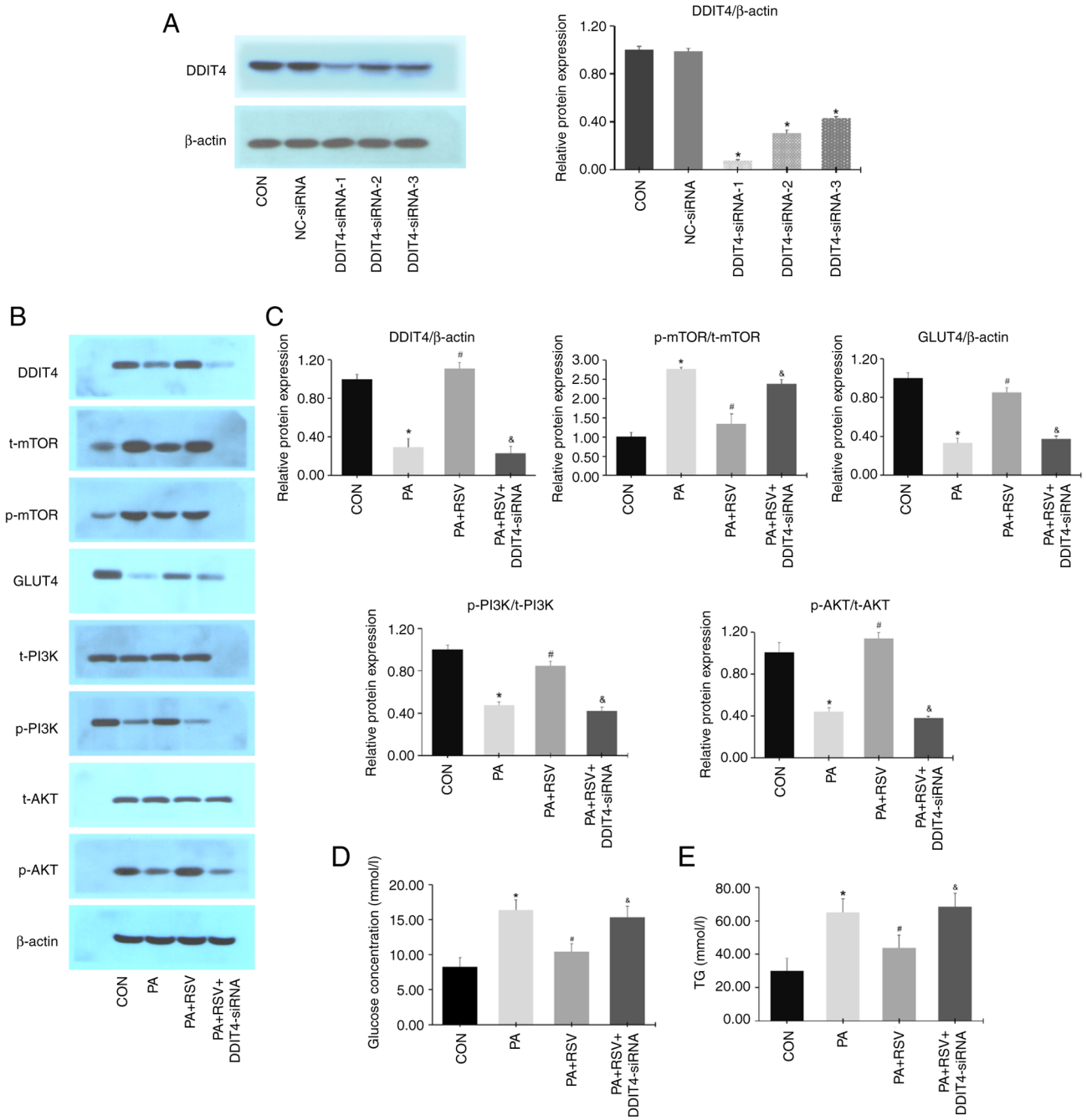

Figure 9. Expression levels of DDIT4, mTOR, GLUT4, PI3K, and AKT in DDIT4-siRNA-treated IR C2C12 cells. (A) DDIT4-siRNA-1 had the most significant silencing effect. (B) Protein expression levels of DDIT4, mTOR, GLUT4, PI3K, and AKT after DDIT4-siRNA treatment. (C) Semi-quantification of p-protein/t-protein ratios for mTOR, PI3K, and AKT and protein expression levels of DDIT4 and GLUT4 after DDIT4-siRNA treatment. (D) Glucose levels in culture medium after DDIT4-siRNA treatment. (E) TG levels of C2C12 cells after DDIT4-siRNA treatment. Data are presented as the mean ± SD (n=3). *P<0.05 vs. the CON group; #P<0.05 vs. the PA group; &P<0.05 vs. the PA + RSV group. DDIT4, DNA-damage-inducible transcript 4; mTOR, mammalian target of rapamycin; GLUT4, glucose transporter 4; PI3K, phosphatidylinositol 3-kinase; AKT, protein kinase B; siRNA, small interfering RNA; IR, insulin resistance; p-, phosphorylated; t-, total; TG, triglyceride; CON, control; PA, palmitic acid; RSV, resveratrol.

alleviating IR in skeletal muscle through modulation of the PI3K/AKT/GLUT4 signaling pathway.

The present study found that the mTOR pathway was activated in mice with HFD-induced IR and in C2C12 cells with PA-induced IR, and that the expression levels of mTOR were increased in skeletal muscle and in C2C12 cells. The continuous activation of the mTOR pathway has been revealed to induce lipid deposition, leading to tissue and cell IR (36,37). The activation of mTOR can trigger a negative feedback pathway involving the downstream signal p70S6K, which when activated leads to the phosphorylation of IRS-1 and promotion of the degradation of IRS-1, thus blocking the PI3K/AKT signal transduction pathway, leading to IR (7). The inhibition of mTOR and p70S6K can inhibit serine phosphorylation of IRS-1 (38), restore the insulin-mediated glucose transport of GLUT4 (39), and improve insulin sensitivity and reduce obesity in mice (40). The present study found that RSV inhibited activation of mTOR, then promoted

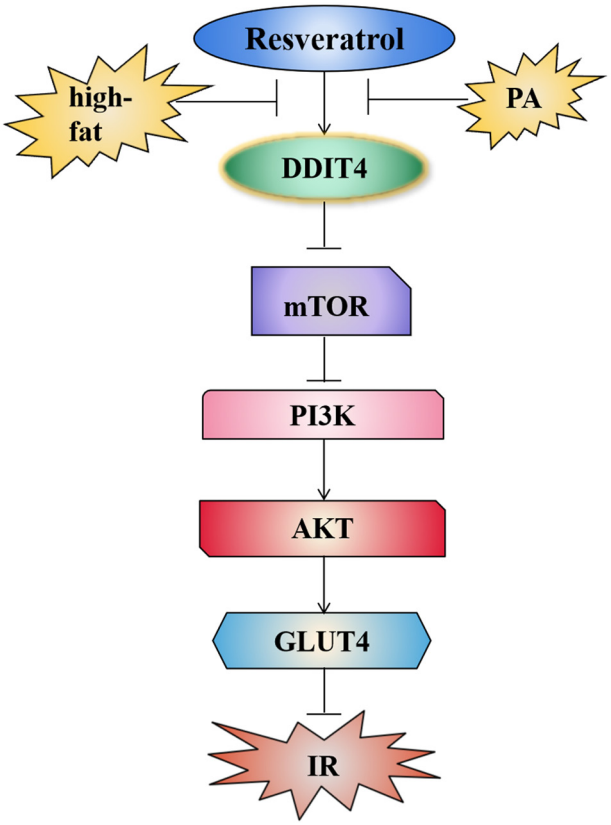

Figure 10. Resveratrol ameliorates IR via the DDIT4/mTOR/PI3K/AKT/GLUT4 pathway. IR, insulin resistance; DDIT4, DNA-damage-inducible transcript 4; mTOR, mammalian target of rapamycin; PI3K, phosphatidylinositol 3-kinase; AKT, protein kinase B; GLUT4, glucose transporter 4; PA, palmitic acid.

the PI3K/AKT/GLUT4 insulin signaling pathway, increased insulin sensitivity and reduced the abnormal glucose and lipid metabolism in PA-treated C2C12 cells and mice fed an HFD.

The present study determined the expression levels of DDIT4, which is a negative regulator of the mTOR signaling pathway (41-43). High expression levels of DDIT4 in rat gastrocnemius muscle cells were demosntrated to inhibit the activity of the mTOR signaling pathway (44). Regazzetti *et al* (45) showed that silencing DDIT4 in 3T3-L1 adipocytes induced an increase in mTOR activity, and inhibited the insulin signaling pathway and adipogenesis in adipocytes. Consistent with the aforementioned studies, the current results indicated that the expression of DDIT4 was inhibited, the expression levels of mTOR and p70S6K were increased, and the PI3K/AKT/GLUT4 insulin pathway was inhibited in mice or C2C12 cells with IR. Wang *et al* (46) found that the expression of DDIT4 was reduced in a rat model of diabetic nephropathy, and the administration of 1,25-dihydroxyvitamin D3 increased DDIT4 expression and caused a significant decrease in the phosphorylation levels of mTOR and p70S6K, resulting in the inhibition of mesangial cell proliferation, hypertrophy, and disordered blood glucose and lipid metabolism (46). Notably, the present study showed that administration of RSV to mice or cells with IR increased the expression of DDIT4, inhibited the mTOR pathway, activated the PI3K/AKT/GLUT4 pathway and reduced the HFD-induced IR, and glucose and lipid metabolism disorders in skeletal muscle and cells. Therefore, RSV may reduce IR by regulating the DDIT4/mTOR signaling pathway.

Limited data from a human-based study revealed that RSV improved insulin sensitivity and fasting glucose levels in patients with type 2 diabetes mellitus and may improve inflammatory status in human obesity (28). A meta-analysis revealed that RSV significantly improved glucose control and insulin sensitivity in individuals with diabetes, but did not affect glycemic levels in nondiabetic individuals (47). A randomized controlled study revealed that RSV treatment improved inflammation, renal function, blood glucose parameters, inflammation, IR, and nutrient sensing systems in elderly patients with type 2 diabetes mellitus, indicating that RSV may be a potential therapeutic drug for the treatment of elderly patients with type 2 diabetes mellitus (48). Another randomized controlled study showed that natural polyphenol, RSV, represents a potential new treatment for management of nonalcoholic fatty liver disease due to its anti-inflammatory and antioxidant properties (49). There is limited research on the mechanism of RSV on IR, as well as glucose and lipid metabolism disorders in human studies. Therefore, in the present study, the mechanism of RSV in improving IR, as well as glucose and lipid metabolism through animal and cell experiments was explored, which generated data for drug preclinical research and laid a foundation for future clinical studies.

Treatment with RSV decreased body weight, blood glucose and lipid levels, and reduced IR in mice. It is proposed that RSV activated the PI3K/AKT/GLUT4 signaling pathway by regulating the DDIT4/mTOR pathway, resulting in significant anti-hyperglycemic and anti-hyperlipidemic activities in skeletal muscle and C2C12 cells. Therefore, RSV can potentially be used as an effective drug for the treatment of type 2 diabetes, as well as a nutritional supplement for the prevention of type 2 diabetes and cardiovascular diseases.

Acknowledgements

Not applicable.

Funding

This study was partially supported by the Scientific Research Project of Hebei Provincial Administration of Traditional Chinese Medicine (grant no. 2023010).

Availability of data and materials

The data generated in the present study may be requested from the corresponding author.

Authors' contributions

XP performed the data collection and analysis and wrote the manuscript. GX, MZ, ZX, DL and ZD performed the sample collection and detection. CW designed the study, performed the primary research, and supported manuscript revision. XP and CW confirm the authenticity of all the raw data. All authors read and approved the final manuscript.

Ethics approval and consent to participate

The present study was approved (approval no. 2023-LW-055) by the Ethics Committee of Hebei General Hospital (Shijiazhuang, China).

Patient consent for publication

Not applicable.

Competing interests

The authors declare that they have no competing interests.

References

1. Zhu X, Wu C, Qiu S, Yuan X and Li L: Effects of resveratrol on glucose control and insulin sensitivity in subjects with type 2 diabetes: Systematic review and meta-analysis. Nutr Metab (Lond) 14: 60, 2017.
2. Duan TT, Hu XB and Cao ZH: Effect of resveratrol in treatment of diabetes mellitus. Prog Microbiol Immunol 48: 99-103, 2020 (In Chinese).
3. Vlavcheski F and Tsiani E: Attenuation of free fatty acid-induced muscle insulin resistance by rosemary extract. Nutrients 10: 1623, 2018.
4. Wang L, Gao P, Zhang M, Huang Z, Zhang D, Deng Q, Li Y, Zhao Z, Qin X, Jin D, *et al*: Prevalence and ethnic pattern of diabetes and prediabetes in China in 2013. JAMA 317: 2515-2523, 2017.
5. Khamzina L, Veilleux A, Bergeron S and Marette A: Increased activation of the mammalian target of rapamycin pathway in liver and skeletal muscle of obese rats: Possible involvement in obesity-linked insulin resistance. Endocrinology 146: 1473-1481, 2005.
6. Tremblay F and Marette A: Amino acid and insulin signaling via the mTOR/p70 S6 kinase pathway. A negative feedback mechanism leading to insulin resistance in skeletal muscle cells. J Biol Chem 276: 38052-38060, 2001.
7. Holz MK, Ballif BA, Gygi SP and Blenis J: mTOR and S6K1 mediate assembly of the translation preinitiation complex through dynamic protein interchange and ordered phosphorylation events. Cell 123: 569-580, 2005.
8. Tinline-Goodfellow CT, Lees MJ and Hodson N: The skeletal muscle fiber periphery: A nexus of mTOR-related anabolism. Sports Med Health Sci 5: 10-19, 2022.
9. Ellisen LW, Ramsayer KD, Johannessen CM, Yang A, Beppu H, Minda K, Oliner JD, McKeon F and Haber DA: REDD1, a developmentally regulated transcriptional target of p63 and p53, links p63 to regulation of reactive oxygen species. Mol Cell 10: 995-1005, 2002.
10. Brugarolas J, Lei K, Hurley RL, Manning BD, Reiling JH, Hafen E, Witters LA, Ellisen LW and Kaelin WG Jr: Regulation of mTOR function in response to hypoxia by REDD1 and the TSC1/TSC2 tumor suppressor complex. Genes Dev 18: 2893-2904, 2004.
11. Reiling JH and Hafen E: The hypoxia-induced paralogs Scylla and Charybdis inhibit growth by down-regulating S6K activity upstream of TSC in Drosophila. Gene Dev 18: 2879-2892, 2004.
12. Wang H, Kubica N, Ellisen LW, Jefferson LS and Kimball SR: Dexamethasone represses signaling through the mammalian target of rapamycin in muscle cells by enhancing expression of REDD1. J Biol Chem 281: 39128-39134, 2006.
13. Jin HO, Seo SK, Woo SH, Kim ES, Lee HC, Yoo DH, An S, Choe TB, Lee SJ, Hong SI, *et al*: Activating transcription factor 4 and CCAAT/enhancer-binding protein-beta negatively regulate the mammalian target of rapamycin via Redd1 expression in response to oxidative and endoplasmic reticulum stress. Free Radical Bio Med 46:1158-1167, 2009.
14. Whitney ML, Jefferson LS and Kimball SR: ATF4 is necessary and sufficient for ER stress-induced upregulation of REDD1 expression. Biochem Biophys Res Commun 379: 451-455, 2009.
15. McGhee NK, Jefferson LS and Kimball SR: Elevated corticosterone associated with food deprivation upregulates expression in rat skeletal muscle of the mTORC1 repressor, REDD1. J Nutr 139: 828-834, 2009.
16. Dennis MD, Coleman CS, Berg A, Jefferson LS and Kimball SR: REDD1 enhances protein phosphatase 2A-mediated dephosphorylation of Akt to repress mTORC1 signaling. Sci Signal 7: ra68, 2014.
17. Williamson DL, Li Z, Tuder RM, Feinstein E, Kimball SR and Dungan CM: Altered nutrient response of mTORC1 as a result of changes in REDD1 expression: Effect of obesity vs REDD1 deficiency. J Appl Physiol (1985) 117: 246-256, 2014.
18. Gordon BS, Steiner JL, Williamson DL, Lang CH and Kimball SR: Emerging role for regulated in development and DNA damage 1 (REDD1) in the regulation of skeletal muscle metabolism. Am J Physiol Endocrinol Metab 311: E157-E174, 2016.
19. Zhang ZM, Liu ZH, Nie Q, Zhang XM, Yang LQ, Wang C, Yang LL and Song GY: Metformin improves high-fat diet-induced insulin resistance in mice by downregulating the expression of long noncoding RNA NONMMUT031874.2. Exp Ther Med 23: 332, 2022.
20. Ayala JE, Samuel VT, Morton GJ, Obici S, Croniger CM, Shulman GI, Wasserman DH and McGuinness OP; NIH Mouse Metabolic Phenotyping Center Consortium: Standard operating procedures for describing and performing metabolic tests of glucose homeostasis in mice. Dis Model Mech 3: 525-534, 2010.
21. Bowe JE, Franklin ZJ, Hauge-Evans AC, King AJ, Persaud SJ and Jones PM: Metabolic phenotyping guidelines: Assessing glucose homeostasis in rodent models. J Endocrinol 222: G13-G25, 2014.
22. Benedé-Ubieto R, Estévez-Vázquez O, Ramadori P, Cubero FJ and Nevzorova YA: Guidelines and considerations for metabolic tolerance tests in mice. Diabetes Metab Syndr Obes 13: 439-450, 2020.
23. Jørgensen MS, Tornqvist KS and Hvid H: Calculation of glucose dose for intraperitoneal glucose tolerance tests in lean and obese mice. J Am Assoc Lab Anim Sci 56: 95-97, 2017.
24. Shu L, Hou G, Zhao H, Huang W, Song G and Ma H: Resveratrol improves high-fat diet-induced insulin resistance in mice by downregulating the lncRNA NONMMUT008655.2. Am J Transl Res 12: 1-18, 2020.
25. Katz A, Nambi SS, Mather K, Baron AD, Follmann DA, Sullivan G and Quon MJ: Quantitative insulin sensitivity check index: A simple, accurate method for assessing insulin sensitivity in humans. J Clin Endocrinol Metab 85: 2402-2410, 2000.
26. Livak KJ and Schmittgen TD: Analysis of relative gene expression data using real-time quantitative PCR and the 2(-Delta Delta C(T)) method. Methods 25: 402-408, 2001.
27. Jensen TL, Kiersgaard MK, Sørensen DB and Mikkelsen LF: Fasting of mice: A review. Lab Anim 47: 225-240, 2013.
28. Barber TM, Kabisch S, Randeva HS, Pfeiffer AFH and Weickert MO: Implications of resveratrol in obesity and insulin resistance: A state-of-the-art review. Nutrients 14: 2870, 2022.
29. Luo J, Chen S, Wang L, Zhao X and Piao C: Pharmacological effects of polydatin in the treatment of metabolic diseases: A review. Phytomedicine 102: 154161, 2022.
30. Ariyanto EF, Danil AS, Rohmawaty E, Sujatmiko B and Berbudi A: Effect of resveratrol in melinjo seed (Gnetum gnemon L.) extract on type 2 diabetes mellitus patients and its possible mechanism: A review. Curr Diabetes Rev 19: e280222201512, 2023.
31. Shahwan M, Alhumaydhi F, Ashraf GM, Hasan PMZ and Shamsi A: Role of polyphenols in combating type 2 diabetes and insulin resistance. Int J Biol Macromol 206: 567-579, 2022.
32. Zhou Q, Wang Y, Han X, Fu S, Zhu C and Chen Q: Efficacy of resveratrol supplementation on glucose and lipid metabolism: A meta-analysis and systematic review. Front Physiol 13: 795980, 2022.
33. Chadt A and Al-Hasani H: Glucose transporters in adipose tissue, liver, and skeletal muscle in metabolic health and disease. Pflugers Arch 472: 1273-1298, 2020.
34. Vlavcheski F, Den Hartogh DJ, Giacca A and Tsiani E: Amelioration of high-insulin-induced skeletal muscle cell insulin resistance by resveratrol is linked to activation of AMPK and restoration of GLUT4 translocation. Nutrients 12: 914, 2020.
35. Kang BB and Chiang BH: A novel phenolic formulation for treating hepatic and peripheral insulin resistance by regulating GLUT4-mediated glucose uptake. J Tradit Complement Med 12: 195-205, 2021.

36. Bar-Tana J: Type 2 diabetes-unmet need, unresolved pathogenesis, mTORC1-centric paradigm. Rev Endocr Metab Dis 21: 613-629, 2020.
37. Bodur C, Kazyken D, Huang K, Tooley AS, Cho KW, Barnes TM, Lumeng CN, Myers MG and Fingar DC: TBK1-mTOR signaling attenuates obesity-linked hyperglycemia and insulin resistance. Diabetes 71: 2297-2312, 2022.
38. Huang SL, Xie W, Ye YL, Liu J, Qu H, Shen Y, Xu TF, Zhao ZH, Shi Y, Shen JH and Leng Y: Coronarin A modulated hepatic glycogen synthesis and gluconeogenesis via inhibiting mTORC1/S6K1 signaling and ameliorated glucose homeostasis of diabetic mice. Acta Pharmacol Sin 44: 596-609, 2023.
39. Den Hartogh DJ, Vlavcheski F, Giacca A and Tsiani E: Attenuation of free fatty acid (FFA)-induced skeletal muscle cell insulin resistance by resveratrol is linked to activation of AMPK and inhibition of mTOR and p70S6K. Int J Mol Sci 21: 4900, 2020.
40. Meng W, Liang X, Chen H, Luo H, Bai J, Li G, Zhang Q, Xiao T, He S, Zhang Y, *et al*: Rheb inhibits beiging of white adipose tissue via PDE4D5-dependent down regulation of the cAMP-PKA signaling pathway. Diabetes 66: 1198-1213, 2017.
41. Dungan CM and Williamson DL: Regulation of skeletal muscle insulin-stimulated signaling through the MEK-REDD1-mTOR axis. Biochem Biophys Res Commun 482: 1067-1072, 2017.
42. Lee Y, Song MJ, Park JH, Shin MH, Kim MK, Hwang D, Lee DH and Chung JH: Histone deacetylase 4 reverses cellular senescence via DDIT4 in dermal fibroblasts. Aging (Albany NY) 14: 4653-4672, 2022.
43. Zhidkova EM, Lylova ES, Grigoreva DD, Kirsanov KI, Osipova AV, Kulikov EP, Mertsalov SA, Belitsky GA, Budunova I, Yakubovskaya MG and Lesovaya EA: Nutritional sensor REDD1 in cancer and inflammation: Friend or foe? Int J Mol Sci 23: 9686, 2022.
44. Murakami T, Hasegawa K and Yoshinaga M: Rapid induction of REDD1 expression by endurance exercise in rat skeletal muscle. Biochem Biophys Res Commun 405: 615-619, 2011.
45. Regazzetti C, Dumas K, Le Marchand-Brustel Y, Peraldi P, Tanti JF and Giorgetti-Peraldi S: Regulated in development and DNA damage responses-1 (REDD1) protein contributes to insulin signaling pathway in adipocytes. PLoS One 7: e52154, 2012.
46. Wang H, Wang J, Qu H, Wei H, Ji B, Yang Z, Wu J, He Q, Luo Y, Liu D, *et al*: In vitro and in vivo inhibition of mTOR by 1,25-dihydroxyvitamin D3 to improve early diabetic nephropathy via the DDIT4/TSC2/mTOR pathway. Endocrine 54: 348-359, 2016.
47. Delpino FM and Figueiredo LM: Resveratrol supplementation and type 2 diabetes: A systematic review and meta-analysis. Crit Rev Food Sci Nutr 62: 4465-4480, 2021.
48. Ma N and Zhang Y: Effects of resveratrol therapy on glucose metabolism, insulin resistance, inflammation, and renal function in the elderly patients with type 2 diabetes mellitus: A randomized controlled clinical trial protocol. Medicine (Baltimore) 101: e30049, 2022.
49. Karimi M, Abiri B, Guest PC and Vafa M: Therapeutic effects of resveratrol on nonalcoholic fatty liver disease through inflammatory, oxidative stress, metabolic, and epigenetic modifications. Methods Mol Biol 2343: 19-35, 2022.